

# DEVELOPMENT OF A HIGH-TEMPERATURE ELECTRON BEAM TEST STAND FOR THERMAL STUDIES OF THE TATTOOS TARGET AT PSI

R. Martinie, R. Eichler, A. Ivanov, S. Jollet, D. Kiselev, M. Mostamand, D. Reggiani, M. Sapinski, J. Snuverink, R. Sobbia, Ph. Spätig, S. Warren  
Paul Scherrer Institute, Villigen, Switzerland

## Abstract

The Targeted Alpha Tumor Therapy and Other Oncological Solutions (TATTOOS) facility at the Paul Scherrer Institute (PSI) will address the growing demand for medically relevant radionuclides using proton-induced spallation at the PSI High Intensity Proton Accelerator (HIPA). The target is designed to operate with a 100  $\mu\text{A}$  - 590 MeV proton beam up to 2400  $^{\circ}\text{C}$  for 2 to 5 weeks. To study the thermal mechanisms critical for the target performance, a high-temperature test stand was developed based on a 60 keV, 100 mA electron beam welding machine. This setup allows heating tantalum foils in vacuum while investigating temperature distributions using a Gaussian beam profile with a rotating frequency up to 1000 Hz. We present here the static and rotating beam profile measurements using a 50  $\mu\text{m}$  tungsten wire scanner moving up to 70 mm/s, with thermionic emission suppressed by voltage biasing. The differences in penetration and energy deposition between 590 MeV protons and 60 keV electrons are discussed to justify the use of electron beam heating as a surrogate for proton irradiation. Finally, preliminary temperature measurements under rotating beam conditions are presented, as well as a preliminary comparison with FEM simulations. Pyrometric measurements show that temperature oscillations remain below 10  $^{\circ}\text{C}$  at 100 Hz for an average temperature of 1715  $^{\circ}\text{C}$ , and preliminary FEM simulations show reasonable agreement with the measurements.

## INTRODUCTION

The Targeted Alpha Tumor Therapy and Other Oncological Solutions (TATTOOS) facility [1] at the Paul Scherrer Institute (PSI) aims to produce radionuclides via proton-induced spallation using the PSI High Intensity Proton Accelerator (HIPA). The production scheme relies on the Isotope Separation On-Line (ISOL) technique [2]: a 100  $\mu\text{A}$ , 590 MeV proton beam [3] impinges on a target heated to temperatures above 2000  $^{\circ}\text{C}$  through both beam power deposition and resistive heating. Neutral spallation products diffuse out of the target material, undergo molecular flow until they reach an ion source, where they are ionized, then accelerated to up to 65 keV, transported as a radioactive ion beam (RIB) and finally mass-separated. ISOL targets have been developed and operated at several facilities, including ISOLDE at CERN [4] and ISAC at TRIUMF [5]. Thermal management is a well-known challenge: temperature homogeneity, cold spots, and heat dissipation capacity directly impact isotope release and target lifetime. Building on this experience, the TATTOOS target baseline consists of thin tantalum foils (25-100  $\mu\text{m}$ ) stacked in a 20 cm long cylindrical

tantalum container, with a total equivalent tantalum thickness of up to 10 cm.

Sustained operation at high temperatures induces thermal ageing mechanisms, such as grain growth, thermal grooving, sintering and creep, that degrade target performance over time. Since the target becomes highly activated during irradiation and requires costly heavy-handling procedures for exchange, extending the target lifetime is a key design objective. This demands a thorough understanding of the thermal environment and its long-term effects on the target materials. To study these thermal mechanisms under controlled conditions, a high-temperature test stand was developed based on the PSI electron beam welding machine. This setup allows heating tantalum samples in vacuum to the relevant temperatures. This article presents the beam characterization using a tungsten wire scanner, preliminary pyrometric temperature measurements under rotating beam conditions, and preliminary FEM validation.

## PROTON VS ELECTRON BEAM DIFFERENCES

Differences between the operational (590 MeV protons) and experimental (60 keV electrons) beam-matter interactions require careful consideration. At 590 MeV, protons penetrate deep into tantalum with a Bragg peak at approximately 17 cm, well beyond the 10 cm equivalent tantalum thickness of the target. MCNP simulations yield between 200 and 300 W/mm in the TATTOOS target, depending on the geometry [6]. In contrast, 60 keV electrons penetrate only a few micrometers into tantalum: according to the ES-TAR [7] CSDA (Continuous Slowing Down Approximation) range of  $1.29 \times 10^{-2} \text{ g/cm}^2$ , electrons penetrate 7.75  $\mu\text{m}$  in tantalum. The electron backscattering coefficient  $\eta_{\text{BSE}}$  at this energy is 50 % [8]. Therefore, the total electron beam power of 6 kW, reduces to approximately 3 kW after backscattering, delivers orders of magnitude more power to a single foil than under proton irradiation.

## EXPERIMENTAL SETUP

### *Electron Beam Welding Machine*

The electron beam welding machine at PSI operates at an energy  $E_{\text{beam}}$  of 60 keV with a maximum current  $I_{\text{beam}}$  of 100 mA. A magnetic focusing lens, controlled by the coil current  $I_{\text{focus}}$ , sets the beam size and a deflection coil steers the beam, enabling circular rotation patterns at frequencies up to 1 kHz. The work table can be displaced horizontally at speeds up to 70 mm/s.

## Beam Profile Scanner

A 50  $\mu\text{m}$  tungsten wire is mounted on the work table and scanned through the beam 150 mm above the table surface. The wire is connected to a Libera current meter capable of measuring currents from nA to 2 mA. A voltage source providing up to 100 V biasing suppresses thermionic emission from the wire at high temperatures.

## Pyrometric Measurement

An Optris CTratio 1M two-color pyrometer with 1 kHz acquisition frequency is used for temperature measurements. The pyrometer is located outside the vacuum chamber in front of the main viewport, at an optical path length of approximately 700 mm. A flat mirror diverts the infrared radiation emitted by the tantalum foil toward the pyrometer sensor head. The measurement spot size at the foil surface is approximately 7 mm diameter. The emissivity slope was set to a constant value of 1.06 following the recommendation of the Optris manual [9]. However, the spectral emissivity ratio of tantalum varies with temperature, introducing a systematic bias in the reported temperatures. A thermocouple-based calibration is planned to determine the appropriate correction.

## BEAM PROFILE CHARACTERIZATION

### Static Beam

Beam profiles were measured by scanning the tungsten wire through the beam at various beam currents and focusing coil settings. Figure 1 shows profiles measured at a focusing current of 800 mA for several  $I_{\text{beam}}$  values. At  $I_{\text{beam}} = 2.5$  mA, the beam is highly collimated. As the beam current increases, the profiles develop broader tails due to space-charge effects. Both Gaussian and Student-t distributions were fitted to the measured profiles. The Student-t distribution captures the heavier tails at high intensity more accurately, but the Gaussian fit provides a sufficiently good description of the core beam and is adopted for the FEM simulations.

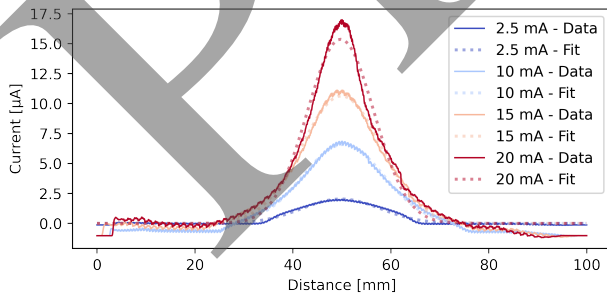


Figure 1: Measured and Gaussian fitted beam profiles for  $I_{\text{focus}} = 805$  mA and  $I_{\text{beam}}$  values of 2.5, 10, 15 and 20 mA.

Figure 2 shows the fitted Gaussian beam size  $\sigma$  as a function of  $I_{\text{beam}}$  and  $I_{\text{focus}}$  currents. These values are interpolated to determine the focusing coil setting required to obtain the desired beam size for temperature investigations. At high

$I_{\text{beam}}$  and low  $I_{\text{focus}}$ , the power density on the wire was sufficient to break it even at the maximum work table scanning speed of 70 mm/s. A dedicated beam profile monitor with higher scanning speeds and thinner wires would extend the characterization to this regime, but the current dataset covers the operating conditions relevant to the thermal studies presented here.

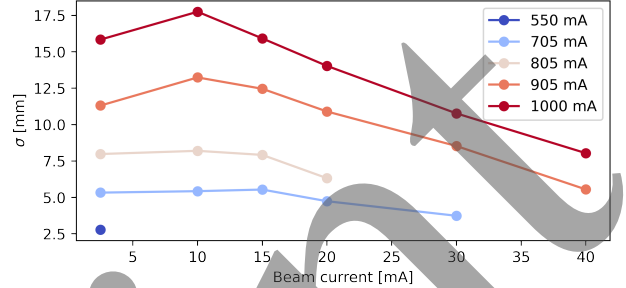


Figure 2: Gaussian beam size  $\sigma$  as a function of beam current  $I_{\text{beam}}$  and the color-coded focusing coil current  $I_{\text{focus}}$ .

### Rotating Beam

When the beam is rotating at radius  $r_0$  with a frequency much higher than the thermal response time of the foil, the time-averaged intensity distribution becomes axisymmetric and is given by [10]:

$$I(r) = \frac{I_{\text{beam}}}{\sigma^2} \cdot \exp\left(-\frac{r^2 + r_0^2}{2\sigma^2}\right) \cdot I_0\left(\frac{r \cdot r_0}{\sigma^2}\right), \quad (1)$$

where  $\sigma$  is the beam width extracted from the static Gaussian fit,  $r_0$  is the rotation radius and  $I_0$  is the modified Bessel function of the first kind. Figure 3 shows a measured rotating beam profile at 1 kHz together with the analytical fit from Eq. (1), showing good agreement.

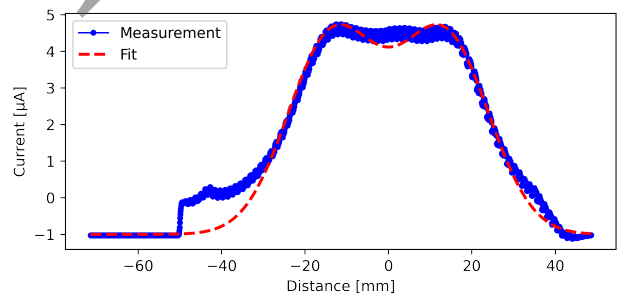


Figure 3: Measured rotating beam profile and fit from Eq. (1) for  $r_0 = 16$  mm  $\sigma = 10$  mm and  $I_{\text{beam}} = 2$  mA.

## PRELIMINARY TEMPERATURE MEASUREMENT

Temperature measurements were performed on a 250  $\mu\text{m}$  thick, 35 mm diameter tantalum foil heated by a rotating beam with a rotation radius of  $r_0 = 10$  mm. For the setpoints of 600 mA focusing coil current and 17 mA beam intensity, the corresponding beam size is  $\sigma = 3$  mm.

Figure 4 shows the temperature time series for rotation frequencies of 1, 2, 10 and 100 Hz. At 1 Hz, the temperature reaches a maximum of 1929 °C with an amplitude of 301 °C. As the rotation frequency increases, the thermal inertia of the foil smoothens out the oscillations: the amplitude decreases to 6.5 °C at 100 Hz for an average temperature of 1715 °C, and the foil approaches a quasi-steady temperature distribution.

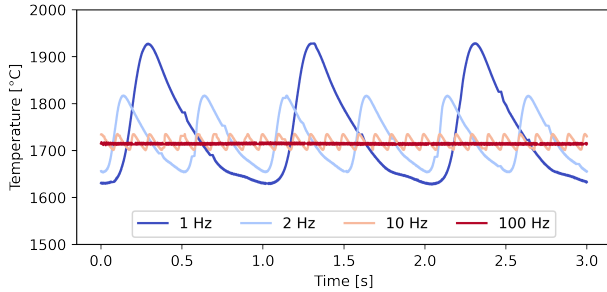


Figure 4: Temperature time series at  $I_{\text{beam}} = 17 \text{ mA}$  and  $r_0 = 10 \text{ mm}$  for rotation frequencies of 1, 2, 10 and 100 Hz.

At 1 Hz, the temperature oscillation exhibits an asymmetric profile, with temperature minima plateauing. This is attributed to foil displacement caused by thermal expansion under the large temperature oscillations, as confirmed by visual observation through the viewport. This highlights the need to mechanically constrain the foil during the measurement. Post-experiment inspection confirmed that the foil had deformed permanently.

## PRELIMINARY FEM COMPARISON

FEM simulations were performed using Ansys<sup>®</sup> Mechanical 2024R2. A transient thermal model of the 250  $\mu\text{m}$  thick, 35 mm diameter tantalum foil was built. Temperature-dependent emissivity from [11] and thermal conductivity from the Granta material database were used. The only boundary condition is radiation on the top face of the foil to the ambient room temperature. A time-dependent internal heat generation term was applied via an APDL script with a time step of 25 ms. The simulation was run for 10 rotation cycles, and the last 3 cycles were extracted after the solution reached periodic steady state. The maximum power density is calculated with:

$$Q_0 = \frac{\eta_{\text{BSE}} \cdot I_{\text{beam}} \cdot E_{\text{beam}}}{2\pi \cdot \sigma^2 \cdot L_{\text{foil}}}, \quad (2)$$

where  $\eta_{\text{BSE}}$  is the backscattering coefficient,  $I_{\text{beam}}$  and  $E_{\text{beam}}$  are the beam current and energy,  $\sigma$  is the Gaussian beam size and  $L_{\text{foil}}$  is the foil thickness. The power density is assumed homogeneous through the foil thickness given the thermally thin regime. The beam center rotates as:

$$x_c = r_0 \cdot \cos(\omega t), \quad y_c = r_0 \cdot \sin(\omega t), \quad (3)$$

and the spatial distribution of the heat source is:

$$Q = Q_0 \cdot \exp\left(-\frac{(x - x_c)^2 + (y - y_c)^2}{2\sigma^2}\right). \quad (4)$$

Figure 5 shows the measured and simulated mean temperature and amplitudes for beam currents ranging from 2 mA to 10 mA. FEM simulations were performed at 4 mA and 10 mA. Good agreement is obtained on mean temperatures: 1409 °C measured versus 1438 °C simulated at 4 mA (2 % difference), and 1708 °C versus 1754 °C at 10 mA (2.7 % difference). However, the simulated amplitudes exceed the measurements by a factor of approximately 1.8, despite averaging the FEM results over the pyrometer spot area. Without spatial averaging, the FEM predicts peak temperatures of 1661 °C at 4 mA and 2285 °C at 10 mA.

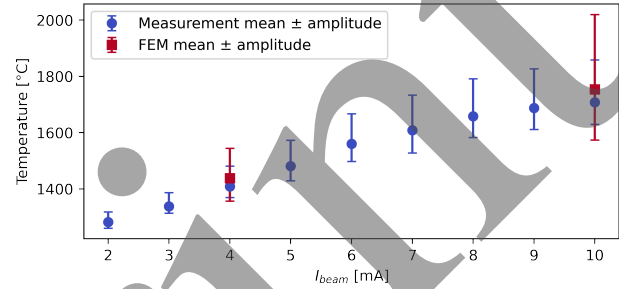


Figure 5: Measured and simulated mean temperature and amplitude as a function of beam current at 1 Hz rotation and  $\sigma = 3 \text{ mm}$ .

It should be noted that this preliminary comparison was performed at an extreme case of 1 Hz rotation, which is far below the 100 Hz to 400 Hz range foreseen for TATTOOS operation, where temperature oscillations become negligible and only the mean temperature is relevant. In this regard, the FEM predictions agree well with the measurements.

## CONCLUSION

A high-temperature electron beam test stand is being developed at PSI for thermal studies of the TATTOOS target. The electron beam was characterized using a tungsten wire scanner, demonstrating Gaussian beam parameters across a wide range of operating conditions. Pyrometric measurements under rotating beam conditions showed that temperature oscillations become negligible above 100 Hz at the average temperature 1715 °C. The preliminary FEM simulations are in good agreement with the mean experimental data. However, the simulated amplitudes exceed the measured ones by a factor 1.8. Future work will focus on mechanical constraints to limit foil movement, thermocouple-based calibration of the pyrometer emissivity slope, and the use of larger beam sizes to reduce averaging effects. Once these features are included, higher temperatures and thermal ageing studies are planned.

## ACKNOWLEDGMENTS

The authors thank the PSI Workshop and especially Samuel Bugmann for his significant help in the operation of the electron beam welding machine and construction of the wire scanner.

## REFERENCES

- [1] R. Eichler *et al.*, “IMPACT conceptual design report”, Paul Scherrer Institut, Rep. PSI Bericht 22-01, 2022.
- [2] M. Huysse, “ISOL techniques, present status and new developments”, *Nucl. Phys. A*, vol. 701, no. 1, pp. 265–271, 2002. doi:10.1016/S0375-9474(01)01595-0
- [3] M. Hartmann, D. Reggiani, J. Snuverink, H. Zhang, and M. Seidel, “High power electrostatic beam splitter for a proton beamline”, *Phys. Rev. Accel. Beams*, vol. 27, no. 2, p. 023502, Feb. 2024. doi:10.1103/PhysRevAccelBeams.27.023502
- [4] S. Rothe *et al.*, “Targets and ion sources at CERN-ISOLDE — facilities and developments”, *Nucl. Instrum. Methods Phys. Res. B*, vol. 542, pp. 38–44, 2023. doi:10.1016/j.nimb.2023.05.058
- [5] P. Bricault, M. Dombsky, A. Dowling, and M. Lane, “High power target developments at ISAC”, *Nucl. Instrum. Methods Phys. Res. B*, vol. 204, pp. 319–324, 2003. doi:10.1016/S0168-583X(03)00504-4
- [6] S. Jollet *et al.*, “Development of the TATTOOS target”, in *Proc. IPAC’23*, Venice, Italy, May 2023, pp. 2526–2529. doi:10.18429/JACoW-IPAC2023-TUPM127
- [7] M. J. Berger, J. S. Coursey, M. A. Zucker, and J. Chang, “ESTAR, PSTAR, and ASTAR: computer programs for calculating stopping-power and range tables for electrons, protons, and helium ions (version 1.2.3)”, National Institute of Standards and Technology, Gaithersburg, MD, Maryland, USA, Rep. NISTIR 4999, 2005.
- [8] F. Akbari, “A comprehensive open-access database of electron backscattering coefficients for energies ranging from 0.1 keV to 15 MeV”, *Med. Phys.*, vol. 50, no. 9, pp. 5920–5929, 2023. doi:10.1002/mp.16604
- [9] *Optris CTratio Operator’s manual*, Optris GmbH, Berlin, Germany, 2024.
- [10] T. Reiss, D. Reggiani, M. Seidel, V. Talanov, and M. Wohlmuther, “Simulation of a beam rotation system for a spallation source”, *Phys. Rev. Spec. Top. Accel. Beams*, vol. 18, no. 4, p. 044701, 2015. doi:10.1103/PhysRevSTAB.18.044701
- [11] N. D. Milošević, G. Vuković, D. Pavičić, and K. Maglić, “Thermal properties of tantalum between 300 and 2300 K”, *Int. J. Thermophys.*, vol. 20, no. 4, pp. 1129–1136, 1999. doi:10.1023/A:1022659005050